On the Function of *N*-[(9-β-D-Ribofuranosylpurin-6-yl)carbamoyl]threonine in Transfer Ribonucleic Acid. Metal Ion Binding Studies†

P. Rabindra Reddy,‡ W. David Hamill, Jr.,§ Girish B. Chheda, and Martin P. Schweizer*

ABSTRACT: The unusual transfer ribonucleic acid (RNA) anticodon adjacent modified nucleoside *N*-[(9-β-D-ribofuranosylpurin-6-yl)carbamoyl]threonine, t^6A, and its N^6-methyl (mt^6A) and 5′-phosphate (pt^6A) derivatives are efficient ligands for magnesium and manganese ions, as demonstrated by potentiometry and nuclear magnetic resonance spectroscopy. Analysis of the ^1H and ^{13}C NMR spectra of t^6A in the presence of paramagnetic Mn(II) at 32–34 °C has shown that the metal ion binds to the carboxyl group and probably N_6 of the side chain as well as the N_1 or N_7 atom of the adenine ring. A more specific and stronger metal–ligand complex between Mn(II) and pt^6A is evident from the ^1H, ^{13}C, and ^{31}P NMR data. In this case, the metal forms a complex involving phosphate, N_7 of the adenine and the carboxyl group, and N_6 of the side chain. Blocking the N_6 site as in mt^6A attenuates the interaction, as revealed in the proton spectra. Potentiometric titrations at 30 °C and in 0.1 M KNO_3 have produced findings parallel to the NMR data on the interaction of Mn(II) with these ligands and have allowed a quantitative comparison between them as well as a comparison of the binding between Mg(II) and Mn(II). The stability constants (log *K*) for 1:1 metal–ligand complexes between Mg(II) and t^6A, mt^6A, and pt^6A are respectively 5.5, 4.3, and 7.1. For Mn(II), the respective values are 6.0, 4.5, and 7.9. In the case of pt^6A, the stability constants are about 5 log *K* units larger than those obtained for Mg(II) and Mn(II) binding to 5′-AMP [Khan, M. M. T., & Martell, A. E. (1967) *J. Am. Chem. Soc. 89*, 5585]. Thus the threonine side chain is an important determinant in the interaction between the modified nucleosides and metal ions, and these results are supportive of the idea that a facet of the function of this type of unusual nucleoside in transfer RNA is as a specific ligand for magnesium ion, a postulate promulgated earlier [Miller, J. P., Hussain, Z., & Schweizer, M. P. (1976) *Nucleic Acids Res. 3*, 1185].

One of the intriguing problems in biochemistry deals with the function of the plethora of unusual compounds found in transfer ribonucleic acid (tRNA) (McCloskey & Nishimura, 1977; Hall, 1971). We have been particularly involved with certain highly modified purine nucleosides located at the 3′ end of the anticodon sequence. In tRNAs which recognize codons beginning with adenosine, the hydrophilic nucleoside *N*-[(9-β-D-ribofuranosylpurin-6-yl)carbamoyl]threonine, t^6A,[1] or its N^6-methyl analogue, mt^6A is located adjacent to the anticodon (Takemura et al., 1969; Kimura-Harada et al., 1972a,b). Although the structure (Chheda et al., 1969; Schweizer et al., 1969) and biosynthesis (Chheda et al., 1972; Powers & Peterkofsky, 1972; Korner & Soll, 1974; Elkins & Keller, 1974) of this compound have been known for some time, its functional role in tRNA remains unexplained. It is likely that no singular role will be uncovered; rather it is likely that multifaceted functions exist. Parthasarathy et al. (1974a,b) have postulated, from X-ray data, that intramolecular hydrogen bonding between the side chain and N_1 of the adenine ring prevents the occurrence of intermolecular Watson–Crick interaction and thus signals the adjacent anticodon sequence. Using model compounds, Korytnyk et al. (1976) have shown the presence of an intramolecular hydrogen bond in Me_2SO solution of the free base of t^6A.

We have shown (Miller et al., 1976) that t^6A is necessary for proper codon–anticodon interaction to occur on ribosomes. In this study, t^6A-deficient [^{14}C]Ile-$tRNA^{Ile}$ bound less extensively to the synthetic isoleucine mRNA, poly(AUC), on ribosomes than did normal t^6A-containing [^{14}C]Ile-$tRNA^{Ile}$, as a function of Mg(II) concentration. This finding suggested that t^6A may be a binding site for Mg(II). In preliminary communications, we have shown by carbon-13 NMR (Schweizer & Hamill, 1978) and potentiometry (Reddy et al., 1979) that t^6A is indeed a ligand of both Mg(II) and the paramagnetic analogue Mn(II). The side chain was shown to be involved in this interaction.

Although it has been observed both in the solid state (Jack et al., 1977; Holbrook et al., 1977; Quigley et al., 1978) and in solution (Bolton & Kearns, 1978) that the anticodon loop region is a "tight" metal ion binding site, there has been little evidence that the unusual anticodon-adjacent nucleosides may be directly involved in this interaction. Thedford & Straus (1974) speculated that Mg(II) bound to the isoprene unit of i^6A, in a homopolymer of this nucleoside. In a more appropriate example, Bolton & Kearns (1978) observed quenching of wyosine (Y nucleoside) fluorescence when europium bound to the anticodon loop area of yeast $tRNA^{Phe}$, implying an interaction either directly with the modified nucleoside or indirectly by effecting a change in loop conformation.

In this paper, we present parallel potentiometric and NMR data on t^6A and its N^6-methyl (mt^6A) and 5′-phosphate (pt^6A) derivatives which serve to illustrate the nature and extent of

† From the Department of Medicinal Chemistry (P.R.R. and M.P.S.) and the Department of Chemistry (W.D.H.), University of Utah, Salt Lake City, Utah 84112, and Department of Biophysics, Roswell Park Memorial Institute, Buffalo, New York 14203 (G.B.C.). *Received November 7, 1980; revised manuscript received April 1, 1981.* Support for this work was derived from U.S. Public Health Service Grants GM25591 (M.P.S.), GM05546 (W.D.H., Postdoctoral Fellowship), CA14185 (G.B.C.), and RR00574 and RR07092 (NMR Regional Resource Grants) to David M. Grant. A preliminary report of this work was presented at the 35th American Chemical Society Northwest Regional Meeting, Salt Lake City, UT, June 12–14, 1980.

‡ Present address: Department of Chemistry, Emory University, Atlanta, GA 30322.

§ Present address: Telephone Service Center, Digital Equipment Corp., Colorado Springs, CO 80919.

[1] Abbreviations used: t^6A, *N*-[(9-β-D-ribofuranosylpurin-6-yl)carbamoyl]threonine; pt^6A, 5′-phosphate of t^6A; mt^6A, *N*-[(9-β-D-ribofuranosylpurin-6-yl)methylcarbamoyl]threonine; Ile-$tRNA^{Ile}$, isoleucine-specific tRNA aminoacylated with isoleucine; i^6A, N^6-(Δ^2-isopentenyl)adenosine; TMAC, tetramethylammonium chloride; Me_4Si, tetramethylsilane; Me_2SO, dimethyl sulfoxide (dmso in figures); EDTA, ethylenediaminetetraacetic acid.

0006-2960/81/0420-4979$01.25/0

metal–ligand interaction. Whereas in the NMR experiments with paramagnetic Mn(II) we can obtain information on the site and extent of binding via loss of peak intensities where ligand/metal ratios are typically 2000–10 000:1, the potentiometric measurements enable quantitative determination of stability constants for binding of both Mg(II) and Mn(II) for equimolar ligand and metal ion concentrations.

Materials and Methods

Ligands. The syntheses of t^6A (and its base), mt^6A, and pt^6A have been described previously (Chheda & Hong, 1971; Dutta et al., 1975). Sodium salts of the nucleotides were prepared by titrating aqueous solutions of the acid forms with 1 equiv of NaOH. Amberlite CG-50 resin (Mallinckrodt), sodium form, was used to convert the barium salt of pt^6A. Chelex 100 resin (Bio-Rad), sodium form, was employed to remove divalent metal ions from these ligands. These materials were stored at −20 °C in the presence of a desiccant.

For every titration, fresh solid ligand was weighed out in order to avoid possible hydrolysis of stock aqueous solutions. Concentrations were 10^{-4} M. Analytical grade metal salts were obtained from Mallinckrodt and were standardized volumetrically by titration with the disodium salt of EDTA in the presence of a suitable indicator as outlined by Schwarzenbach (1975). Potentiometric titration of the ligand was carried out with a standard sodium hydroxide (carbonate free) solution in the absence and presence of the metal ion being investigated. The ionic strength was maintained constant by using 0.10 M KNO_3 as the supporting electrolyte and relatively low concentrations of ligand and metal ion at a concentration ratio of 1:1. A stream of nitrogen was passed through the titration cell in order to exclude atmospheric CO_2. All titrations were carried out at 30 ± 0.1 °C by use of a Brinkman Laude K-2/R thermostated circulator.

A Sargent-Welch pH meter with combination electrode was used to determine the hydrogen ion concentration. The electrode system was calibrated by direct titration of acetic acid, and the observed pH meter reading was compared to the actual hydrogen ion concentration determined from the pK_a value of acetic acid at 30 °C, as tabulated by Harned & Owen (1959). The pH regions below 3.5 and above 10.5 were calibrated by measurements in HCl and NaOH solutions, respectively.

pK Values of mt^6A and pt^6A [t^6A Is Treated in Reddy et al. (1979)]. The acid dissociation constant of mt^6A (HL^-) is related to the usual equilibrium expression:

$$HL^- \rightleftharpoons L^{2-} + H^+ \quad \ldots \qquad (1)$$

In the case of pt^6A (H_3L^{2-}; refer to Scheme I for structures and dissociations), there are three equations corresponding to the three separate dissociations:

$$H_3L^{2-} \overset{K_a}{\rightleftharpoons} H_2L^{3-} + H^+ \qquad (2)$$

$$H_2L^{3-} \overset{K_{2a}}{\rightleftharpoons} HL^{4-} + H^+ \qquad (3)$$

$$HL^{4-} \overset{K_{3a}}{\rightleftharpoons} L^{5-} + H^+ \qquad (4)$$

The constant K_a for mt^6A and constants K_a, K_{2a}, and K_{3a} for pt^6A were calculated by a direct algebraic method.

Binding Constants. In the titration of pt^6A with equimolar amounts of Mg(II) or Mn(II) ion (Figure 8), a steep inflection resulted at $a = 2$ (where a = moles of base added per mole of pt^6A), indicating the formation of a 1:1 metal–ligand complex in solution. The assumption of simultaneous formation of both protonated and 1:1 chelate species gave negative

Scheme I: Schematic Representation of the Hydrogen Dissociations from pt^6A[a]

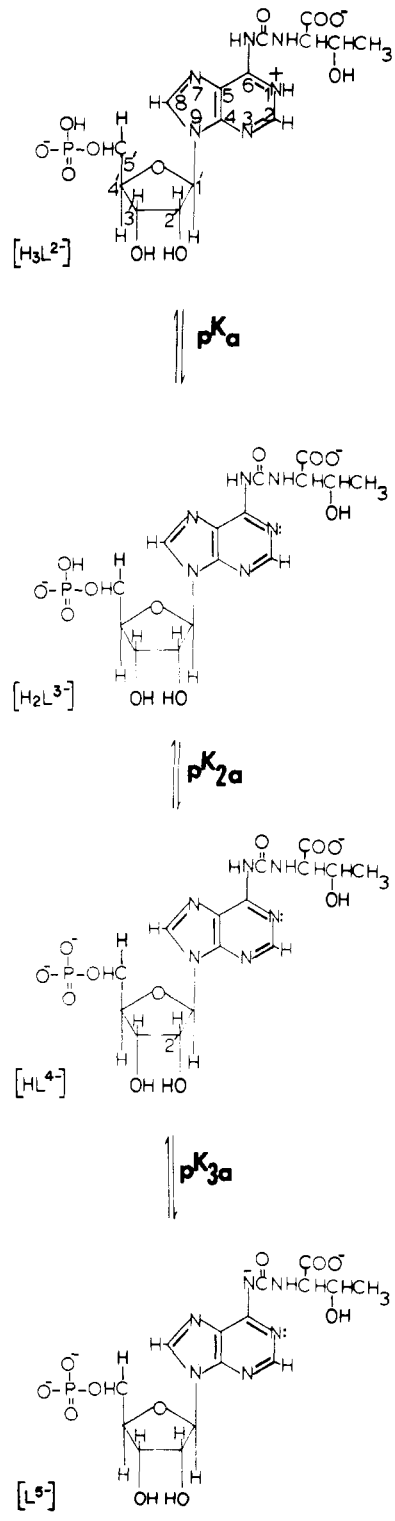

[a] At pH 4, there is a partial positive charge, δ^+, at N_1 (although N_3 and N_7 are less basic than N_1, there is also undoubtedly some protonation at these sites at this pH) so that pt^6A has a net negative charge (between 1.5 and 2). Therefore pt^6A at pH 4 is designated as $[H_3L^{2-}]$. pt^6A with N_1 deprotonated is denoted H_2L^{3-} to illustrate this dissociation. The actual charge on the molecule is 2.

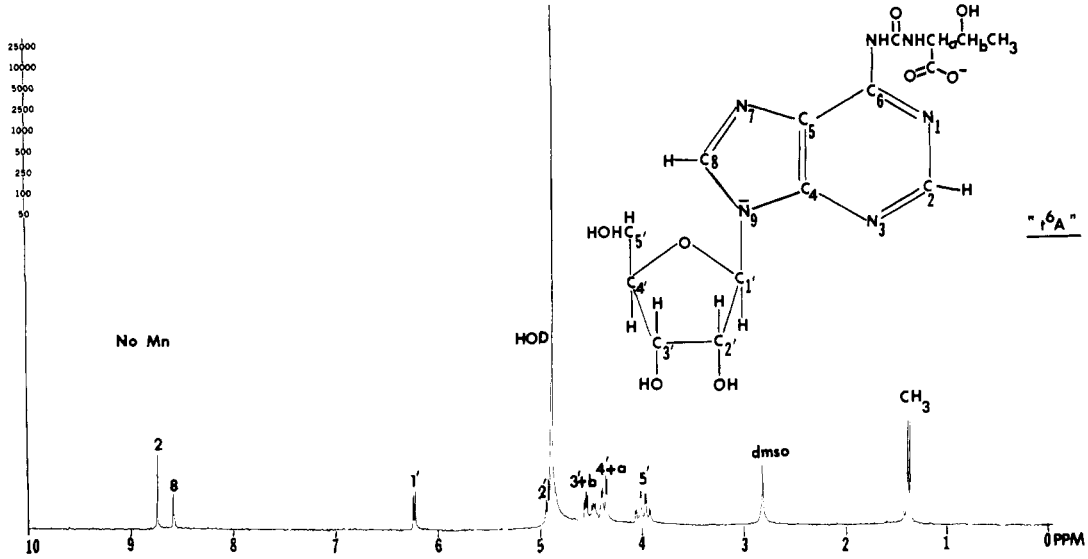

FIGURE 1: 300-MHz proton spectrum of 0.036 M t^6A in D_2O, 3-kHz sweep width, and 200 transients.

results. Therefore the following equations were used to calculate the binding constants of the interaction of metal ion with pt^6A.

$$M^{2+} + L^{5-} \overset{K_1}{\rightleftharpoons} ML^{3-} \quad (5)$$

$$K_1 = [ML^{3-}]/([M^{2+}][L^{5-}])$$

Related equilibria may be defined as

$$M^{2+} + H_2L^{3-} \rightleftarrows ML^{3-} + 2H^+ \quad (6)$$

A buffer region found between $a = 2$ and $a = 3$ probably involves the disproportionation of the 1:1 chelate:

$$2ML^{3-} + 2OH^- \rightleftarrows ML_2^{8-} + M(OH)_2 \quad (7)$$

The following expressions may be written for the 1:1 complex between $a = 0$ and $a = 2$. If T_L represents the total concentration of various ligand species and T_m that of all metal species, then

$$T_L = [H_3L^{2-}] + [H_2L^{3-}] + [HL^{4-}] + [L^{5-}] + [ML^{3-}] \quad (8)$$

$$T_M = [M^{2+}] + [ML^{3-}] \quad (9)$$

The total titrable hydrogens are

$$[H^+] = [H_2L^{3-}] + [HL^{4-}] + [L^{5-}] + [ML^{3-}] - T_L + [OH^-] \quad (10)$$

When suitable material balance equations are solved, K_1 can be obtained from the potentiometric data with the help of eq 5.

The equilibrium involved in metal chelate formation in the titrations of mt^6A with metal ions at a ratio of 1:1 can be written as

$$M^{2+} + L^{2-} \overset{K_1}{\rightleftharpoons} ML \quad (11)$$

$$K_1 = [ML]/([M^{2+}][L^{2-}])$$

and for t^6A as

$$M^{2+} + L^{3-} \overset{K_1}{\rightleftharpoons} ML^- \quad (12)$$

$$K_1 = [ML^-]/([M^{2+}][L^{3-}])$$

Here L^{3-} represents t^6A with negative charge at the carboxyl and N_6 and deprotonated at N_1. The K_1's were calculated with the help of eq 11 and 12.

Nuclear Magnetic Resonance. Sodium salts of the various ligands were dissolved in D_2O (Stohler; 99.8% D) or H_2O, both ascertained by atomic absorption to be free of paramagnetic impurities. For proton NMR measurements of metal–ligand interactions, the concentrations of t^6A, mt^6A, and pt^6A were 0.036 M in 0.3 mL of D_2O. $MnCl_2$ (Baker) in D_2O was dispensed from a precision 2-μL Hamilton syringe right into the 5-mm NMR sample tube. Most proton spectra were recorded on a Varian SC-300 high-field spectrometer operating at 300 MHz, although Varian EM390 and XL-100 spectrometers were also used. TMAC was used as an internal chemical shift reference. Sample concentrations for ^{13}C NMR measurements were 0.3–0.5 M. ^{13}C spectra were recorded at 25 and 75 MHz on XL-100 and SC-300 spectrometers, respectively, operating in the FT mode. Chemical shifts were measured from internal dioxane and converted to Me_4Si by adding 66.3 ppm. Probe temperatures were controlled at 32–34 °C.

Results

Spectral Assignments. The 300-MHz spectrum of 0.036 M t^6A in D_2O is presented in Figure 1. Due to the ease of exchange of H_8 by heating in D_2O (Schweizer et al., 1964), this proton was readily discriminated from H_2. From the intensities of H_2 and H_8 in Figure 1, it can be seen that partial deuteration has occurred at C_8. Homonuclear $^1H\{^1H\}$ decoupling experiments facilitated the assignment of the four complex patterns between the HOD and $H_{5'}$, $H_{5''}$ peaks. From low to higher field, these are $H_{3'}$, H_b, $H_{4'}$, and H_a. All other peaks are readily assigned by comparison with typical nucleosides. The various vicinal and geminal furanose coupling constants are given in Table I.

By comparison with t^6A, the ^1H spectrum of mt^6A is readily assigned as in Figure 5. The differences are the N_6–CH_3 singlet at 3.8 ppm and the coalescence of H_b and $H_{4'}$ patterns plus the presence of the internal chemical shift reference TMAC. This reference was also used for pt^6A (Figure 6).

The monophosphate exists primarily in the antiglycosidic conformation (Schweizer et al., 1968), and in this conformation the deshielding influence of the phosphate dianion on the H_8 proton is evident in the reversal of the relative position of H_8 and H_2 (Figure 6). The assignment was confirmed by deuteration at C_8.

Solution Properties of t^6A. (i) Preferred Conformation. Table I contains the various vicinal C–H and H–H coupling

Table I: t⁶A Coupling Constants (Hz) and Chemical Shifts (ppm) from Me_4Si

(A) C–H Coupling Constants and ^{13}C Chemical Shifts[a] Measured at 75 MHz

	$^3J_{C-H}$	δ		$^1J_{C-H}$	δ
CO_2^-		177.69	C_2–H_2	198.8	151.90
C(=O)–H_b	2.64	155.98	C_8–H_8	218.1	
C_6–H_2	10.25	150.46	$C_{1'}$–$H_{1'}$	163.2	89.31
C_6–H_8	10.25		$C_{4'}$–$H_{4'}$	149.5	86.42
C_4–H_2	11.3	149.92	$C_{2'}$–$H_{2'}$	150.5	74.75
C_4–H_8	11.3		$C_{3'}$–$H_{3'}$	176.9	71.27
C_4–$H_{1'}$	2.87		C_b–H_b	145.8	69.10
C_8–$H_{1'}$	2.81	141.71	$C_{5'}$–$H_{5'}$	143.1	62.22[c]
C_5–H_8	11.3[b]	120.71	C_a–H_a	142.9	62.22

(B) $^3J_{H-H}$ Coupling Constants Measured at 300 MHz

$H_{1'}$–$H_{2'}$	5.4	$H_{4'}$–$H_{5''}$[d]	3.6
$H_{2'}$–$H_{3'}$	5.4	$H_{5'}$–$H_{5''}$	(−)12.7
$H_{3'}$–$H_{4'}$	3.7	H_a–H_b	3.7
$H_{4'}$–$H_{5'}$[d]	2.7	CH_3–H_b	6.5

[a] Schweizer & Hamill (1978). [b] Measured at 25 MHz. [c] $C_{5'}$ and C_a are overlapped. [d] Indicates 5′-methylene proton resonance at lower field, 5″ to higher field.

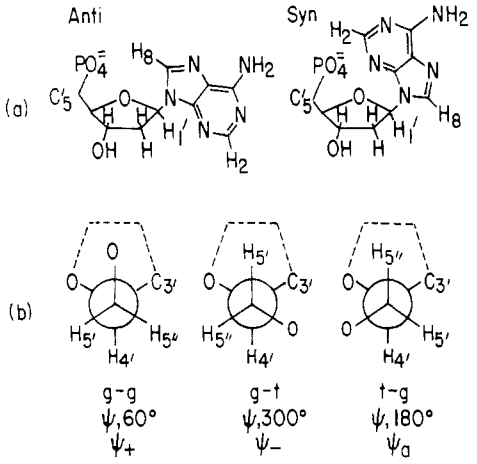

FIGURE 2: (a) Anti (left) and syn (right) conformations about the glycosidic bond illustrated for 5′-AMP. (b) Staggered rotomeric conformations about the $C_{4'}$–$C_{5'}$ bond.

constants extracted from first-order continuous wave 300-MHz ^1H spectra of t⁶A taken over narrow sweep widths (ca. 500 Hz). We may use these coupling constants to obtain an idea of the preferred time-average solution conformation of t⁶A by relating them to the various dihedral angles, θ, between the interacting atoms via the well-known relationship first described by Karplus (1959), $J = A\cos^2\theta - B\cos\theta + C$, where the constants are associated with the nature of the substituents attached to members of the dihedral interaction. Davies (1978) has written a comprehensive review of nucleoside and nucleotide conformations in which this methodology has been evaluated.

For some time the realization has existed that ribofuranose rings exist in an equilibrium mixture of puckered forms (Hruska et al., 1970; Altona & Sundaralingam, 1973) at room temperature, the features of which may be described through consideration of $J_{1'-2'}$ and $J_{3'-4'}$. The equilibrium between 2′-endo (^2E or S) and 3′-endo (^3E or N) can be approximated by $K_{eq} \simeq J_{1'-2'}/J_{3'-4'}$ (Davis, 1978; Lee et al., 1976). From Table I, K_{eq} ($^2E/^3E$) = 1.46 or 60% ^2E (S), e.g., a slight preference for the 2′-endo pucker for the ribose ring in t⁶A.

The amount of gauche–gauche (*gg*) rotamer of the exocyclic hydroxymethyl group in comparison with trans–gauche (*tg*) and gauche–trans (*gt*) from Figure 2b can be estimated from the empirical relationship (Lee et al., 1976) % *gg* = 13.7 − Σ/9.7, where $\Sigma = {}^3J_{H_{4'}-H_{5'}} + {}^3J_{H_{4'}-H_{5''}}$. For t⁶A, *gg* = 76%.

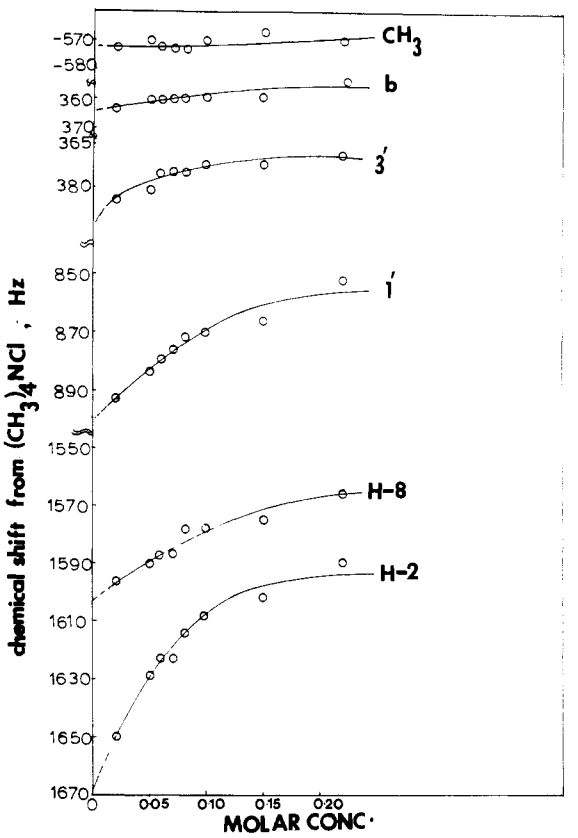

FIGURE 3: Concentration dependence of proton chemical shifts for t⁶A in D_2O, pD 5.3.

Both vicinal C–H coupling constants $^3J_{C8-H_{1'}}$ and $^3J_{C_4-H_{1'}}$, which can be used to determine the relative positions of base and sugar ring, are small, 2.81 and 2.87 Hz, respectively. This means that the torsional angle, XCN, is relatively small and that the preferred glycosidic conformation is either classically anti or syn (Figure 2a) or an equilibrium with both forms equally populated. For the monophosphate, pt⁶A, our ^1H results described below show that the preferred glycosidic conformation is anti.

(ii) Self-Association of t⁶A. We have investigated t⁶A proton chemical shifts vs. concentration (Figure 3) as a means of assessing tendencies toward self-association, as has been found for other purine nucleosides (Broom et al., 1967). Previous work has illustrated that the hypermodified residues as found in tRNA affect stacking properties of oligomers (Schweizer et al., 1971; Watts & Tinoco, 1978; Dea et al., 1978). Formation of stacked aggregates which form and break up rapidly on an NMR time scale is manifested in shifts to higher field with concentration as neighboring diamagnetic adenine rings shield nearby protons. As may be seen in Figure 3, the site of interaction is mainly at the pyrimidine portion of the adenine ring since the upfield shift is largest at H_2, followed by $H_{1'}$ and H_8. The effect is considerably less at $H_{3'}$, and it is apparent that the threonine side chain is not inserted into the stacks since H_b and CH_3 are unaffected. Compared with 2′-deoxyadenosine (Broom et al., 1967), the differential results for H_2, H_8, and $H_{1'}$ are quite similar, and it is likely that t⁶A forms aggregates with adenine rings stacked with the H_2 regions most completely overlapped and with the hydrophilic side chains protruding into the solvent. The magnitudes of the H_2, $H_{1'}$, and H_8 shift changes seen for t⁶A are respectively 78%, 61%, and 55% of those found for 2′-deoxyadenosine over the same concentration range (Broom et al., 1967). Thus the side chain is interfering with the stacking interaction,

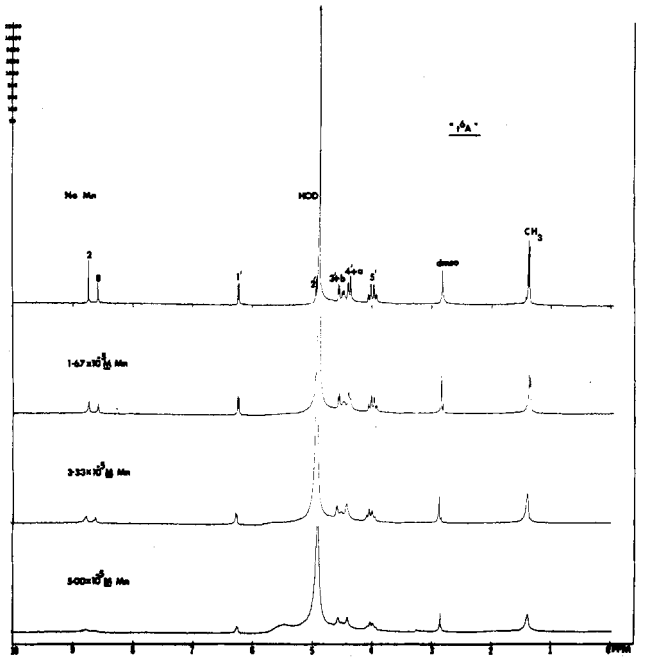

FIGURE 4: 300-MHz proton spectrum showing the titration of 0.036 M t^6A in D_2O with Mn(II) at pD 7.9, 3-kHz sweep width, and 200 transients.

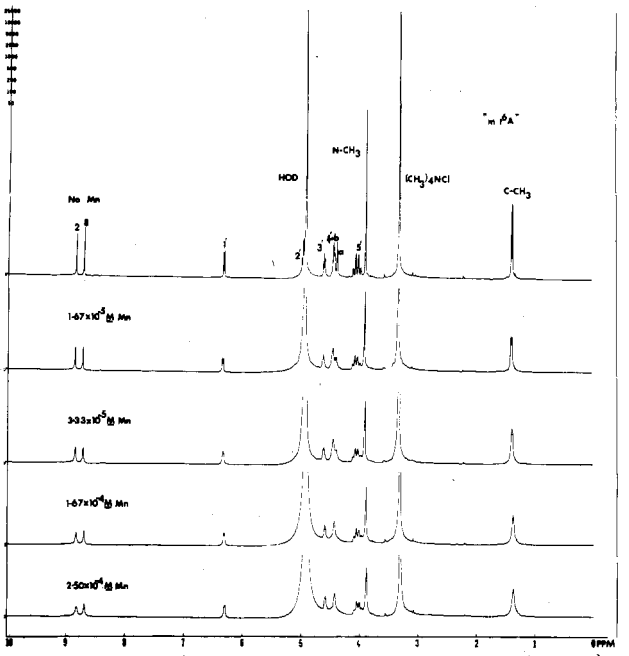

FIGURE 5: 300-MHz proton spectrum showing the titration of 0.036 M mt^6A in D_2O with Mn(II) at pD 7.9, 3-kHz sweep width, and 200 transients.

undoubtedly due to replusion between carboxylate anions.

Interaction of Ligands with Mn(II) and Mg(II)—NMR Results. (i) Carbon-13 NMR Data on t^6A. Our initial studies on the interaction of metal ions with t^6A were concerned with Mn(II) as a paramagnetic analogue of Mg(II), and the binding was followed by ^{13}C NMR (Schweizer & Hamill, 1978). When quantities of Mn(II) were progressively added to 0.5 M t^6A in H_2O, the carboxyl carbon was most drastically broadened first, with C_5 and NHC(=O)NH next sensitive, followed by C_4, C_6, C_a, and C_b. C_2 and C_8 were influenced at higher levels. Ribose carbon peaks and the side chain methyl carbon signal were relatively unaffected during this titration. These results allow a qualitative model of the metal–t^6A interaction to be postulated. The paramagnetic relaxation caused by the dipolar coupling of the spin of the unpaired electron on the metal with ^{13}C nuclear spins has a $1/r^6$ dependence on distance (Carrington & McLachlan, 1967). Thus it is readily apparent that Mn(II) coordinates with the carboxyl group and that a population distribution of secondary sites includes N_1 and N_7 of the adenine ring and/or N_6 and the carbonyl oxygen.

(ii) Proton NMR. We have followed the effects of progressive addition of Mn(II) on the 300-MHz proton NMR spectrum of t^6A (Figure 4). Between the HOD and Me_2SO peaks, the resonances from low to high field are assigned to $H_{3'}$, H_b, $H_{4'}$, H_a, and $H_{5'}$, $H_{5''}$. Adenine ring protons and side chain protons H_a, H_b, and to a lesser extent CH_3 are specifically affected by the initial aliquot of metal ion. All of these resonances except the methyl peak eventually disappear with further Mn(II) addition, and general paramagnetic broadening is seen throughout. These results reinforce the carbon-13 data that metal coordination sites are located on both the side chain and the adenine ring. The solution pD was 7.9 for this titration, so that the N_6–H is partially ionized and the resulting anion may provide a metal coordination site.

(iii) Proton NMR Results on mt^6A. In contrast to the 300-MHz proton NMR results on the addition of Mn(II) to t^6A, the same experiment with mt^6A (Figure 5) yielded much less of an effect by the paramagnetic ion, particularly upon the adenine H_2 and H_8 resonances. In this spectrum, H_b and

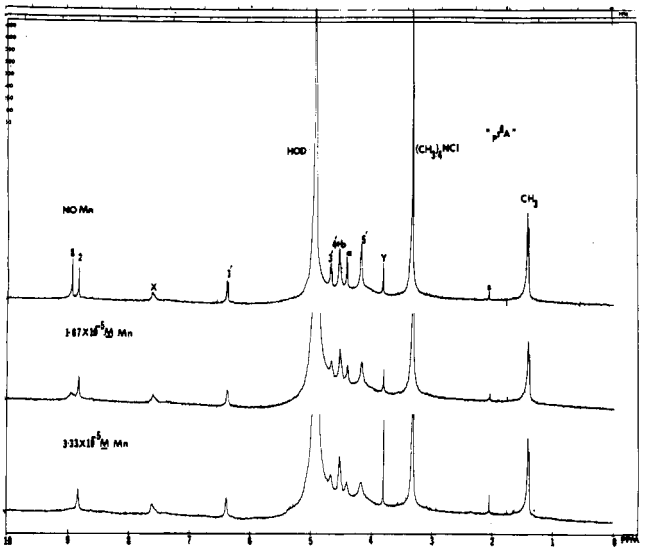

FIGURE 6: 300-MHz proton spectrum showing the titration of 0.036 M pt^6A in D_2O with Mn(II) at pD 7.9, 3-kHz width, and 200 transients. X and Y are unknown impurities. The SC-300 spectrometer was retuned during the sweep of the bottom spectrum, yielding the sharper methyl signal.

$H_{4'}$ are combined, with $H_{3'}$ and H_a, respectively, found to the low- and high-field sides of this combined pattern. As Mn(II) is added, H_b and H_a gradually disappear. This result, when coupled with the lower sensitivity of adenine ring protons, indicates that metal ion is binding to the side chain but the coordination to sites on the base is less extensive compared with t^6A.

Substitution of the N_6–H by a methyl group thus appears to have two effects: (1) at this same pD (7.9), anion formation and, hence, a potential ligand site are blocked; (2) the relative position of the threonine side chain and the adenine ring may be altered such that binding to N_7 and/or N_1 is hindered. Since the metal is not coordinating to N_6, this may have an effect on the lowered interaction with the ring nitrogens.

(iv) ^1H NMR Studies with pt^6A. In order to identify the Mn(II) binding sites on pt^6A, we have monitored the inter-

Table II[a]

Proton Dissociation Constants (pK's) of t^{6}A,[b] mt^{6}A, and pt^{6}A

ligand	pK N_1H	N_6H	PO_3^-H
t^{6}A	3.35 ± 0.01	8.55 ± 0.02	
mt^{6}A	3.36 ± 0.01		
pt^{6}A	3.57 ± 0.01	8.96 ± 0.04	6.16 ± 0.02

Equilibrium Constants for the Interaction of Mn(II) and Mg(II) with t^{6}A,[b] mt^{6}A, and pt^{6}A

metal ion	log K_1[c] t^{6}A[b]	mt^{6}A	pt^{6}A
Mn(II)	6.0	4.5	7.9
Mg(II)	5.5	4.3	7.1

[a] t = 30 °C, and ionic strength = 0.10 M KNO_3. [b] Values taken from Reddy et al (1979). [c] The constants are accurate to ±0.1 log K unit.

action at pD 7.9 by ^{1}H NMR at 300 MHz. The data in Figure 6 serve to illustrate that the interaction of Mn(II) is much stronger with pt^{6}A than with t^{6}A (Figure 4). For instance, at 3.33 × 10^{-6} M Mn(II) both ligands at 0.036 M), the H_8 line in pt^{6}A has disappeared whereas H_8 and H_2, while markedly diminished, are still present in t^{6}A. Significantly in pt^{6}A, H_8 is much more sensitive to metal addition than is H_2, which is indicative of a more specific interaction in the case of pt^{6}A. 5′-Monophosphates in solution generally show a preference for the anti glycosidic conformation (Schweizer et al., 1968), and such is apparently the situation for pt^{6}A, in light of the data in Figure 6.

It is of interest to note the much narrower $H_{5'}$, $H_{5''}$ pattern in pt^{6}A compared to the nucleosides. This behavior may be due to the rotational averaging, about the $C_{4'}$–$C_{5'}$ bond, of $H_{5'}$, $H_{5''}$ chemical shift nonequivalence.

At pD 10.3 the Mn(II)–pt^{6}A interaction is different than that at pD 7.9. The relaxation effects on the proton lines seen at pD 7.9 with 1.67 × 10^{-5} M Mn(II) (Figure 6) are not achieved at pD 10.3 unless the metal/ligand ratio is 10 times greater. The weaker binding at the higher pD may be interpreted in terms of the disproportionation of the 1:1 Mn(II)–pt^{6}A complex (eq 7) into a 2:1 ligand–metal complex in which the interaction is weaker.

(*v*) *^{13}C NMR Data on pt^{6}A.* As expected, the threonine side chain is involved in the coordination of the metal ion, as may be seen by the effect on H_α in Figure 6. Much more dramatic evidence for side-chain interaction is found in the carbon-13 analysis of 0.3 M pt^{6}A as a function of Mn(II) addition. The CO_2^- and NHC(=O)NH peaks of the side chain (as well as C_5 and C_8) are significantly relaxed by the presence of Mn(II), at lower metal/ligand ratios than for t^{6}A (Schweizer & Hamill, 1978). C_8 is definitely more affected than C_2, in contrast to the situation with t^{6}A where both carbon signals responded equivalently. Here again is evidence for a more specific metal–ligand interaction for pt^{6}A.

(*vi*) *^{31}P Results on pt^{6}A.* We have monitored the ^{31}P resonance of pt^{6}A at 40.5 MHz as a function of Mn(II) addition. To a 0.36 M pt^{6}A solution (D_2O, pD 7.9) we added aliquots of the metal over the range 8.5 × 10^{-6}–9.2 × 10^{-5} M. The ^{31}P peak height was reduced ~80% at the highest level. Thus compared with ^{13}C and ^{1}H nuclei, the phosphorus nucleus is most affected at lower [Mn(II)]/[pt^{6}A] ratios.

Potentiometric Results on Metal–Ligand Interaction. (*i*) *t^{6}A.* A more quantitative idea of the ligand–Mn(II) interactions and a comparison with Mg(II) can be obtained by using potentiometric titrations. Preliminary results on t^{6}A were described in Reddy et al. (1979). The constants for proton dissociation from N_1 (pK_a) and N_6 (pK_{2a}) of t^{6}A are given in Table II. The value for pK_a is similar to that of adenosine, and titrations with mt^{6}A show that the second ionization of the t^{6}A is due to N_6–H since the methylated derivative has no dissociation in this pH range.

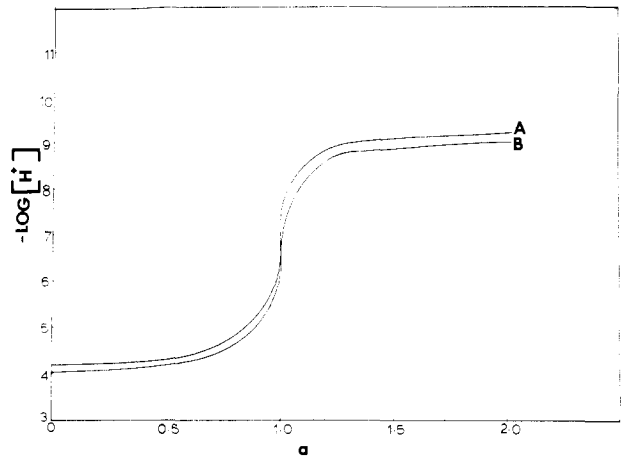

FIGURE 7: Potentiometric titration of mt^{6}A with Mn(II) at a 1:1 ratio of ligand to metal ion, t = 30 °C, and ionic strength = 0.10 M KNO_3. (A) Free mt^{6}A; (B) Mn(II) + mt^{6}A; a = moles of base added per mole of mt^{6}A.

Both Mn(II) and Mg(II) form 1:1 metal–ligand complexes with t^{6}A at the pH when N_1 is protonated (pH 3.35) and when N_6–H dissociates (pH 8.55). At the lower pH, the stability constants for the protonated 1:1 complexes are essentially the same for both metals [log K^M_{MHL} = 3.9 for Mn(II) and 3.8 for Mg(II)]. For the normal 1:1 complexes (ML) formed at the higher, more physiologically relevant pH (eq 12), the binding constant (log K_1) in the case of Mn(II) was 0.5 log K unit higher (Table II); thus the two systems are not entirely analogous, although it is reasonable to suppose that the ligand sites are equivalent for both metal ions. Both constants are considerably higher for the normal than for the protonated complexes, indicative of tighter binding.

(*ii*) *mt^{6}A.* Figure 7 contains titration curves for mt^{6}A in the absence (A) and presence (B) of Mn(II). Both curves give steep inflections at a = 1 (a = moles of NaOH added per mole of ligand), due to the dissociation of N_1–H (the pK_a for the ligand itself is 3.36; Table II). Because of the absence of a hydrogen at N_6, no dissociation was seen at pH ~ 8.5. The interaction of metal with mt^{6}A in the region a = 0 to a = 1 can be expressed as in eq 11. The stability constants are given in Table II. As reinforcement of the proton NMR results, it is evident that the binding of both metal ions is considerably less than that for t^{6}A (~1.2–1.5 log units lower), presumably due to the blocked N_6 site.

(*iii*) *pt^{6}A.* Finally, we have studied the titration of pt^{6}A with metal ions. This ligand is, of course, more relevant to the situation in tRNA because of the presence of the phosphate group, a strong potential binding site.

In Figure 8C is presented the titration of pt^{6}A with base. The two inflections at a = 1 and 2 followed by a buffer region represent respective deprotonations from N_1–H, secondary phosphate, and N_6–H. These equilibria are illustrated in Scheme I. The dissociation constants are listed in Table II. Figure 8D is the titration curve for pt^{6}A in the presence of Mg(II). A similar curve was obtained for Mn(II). The inflection at a = 2 suggests the formation of a 1:1 metal–ligand complex between a = 0 and a = 2 according to eq 5.

The stability constants log K_1 for pt^{6}A plus Mn(II) and Mg(II) are given in Table II. As might be expected, the

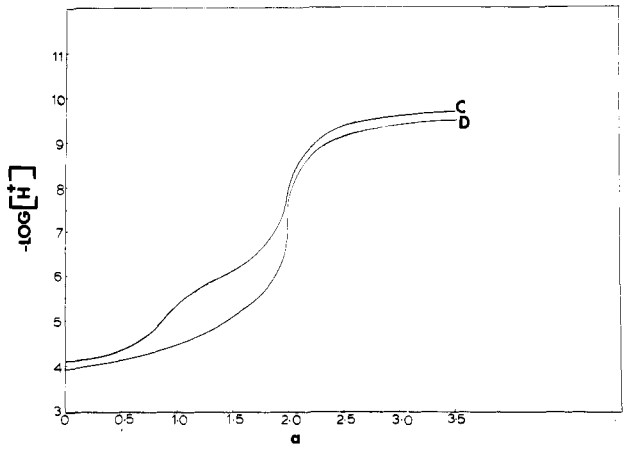

FIGURE 8: Potentiometric titration of pt^{6}A with Mg(II) at a 1:1 ratio of ligand to metal ion, t = 30 °C, and ionic strength = 0.10 M KNO_3. (C) Free pt^{6}A; (D) Mg(II) + pt^{6}A; a = moles of base added per mole of pt^{6}A.

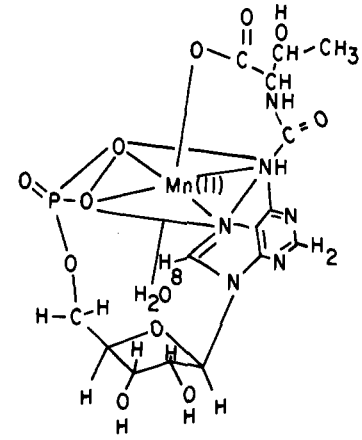

FIGURE 9: Tentative structure for the 1:1 metal complex of Mn(II) with pt^{6}A. The phosphate oxygens, with N_7 and N_6 of the adenine ring, are coordinated in the metal plane. At one apex of the octahedron, the carboxyl group of the threonine side chain is bound, while a water molecule is liganded to the other apex. The glycosidic conformation is anti, and the ribose ring is in the 2′-endo conformation.

monophosphate forms stronger complexes with Mn(II) and Mg(II) than t^{6}A or mt^{6}A due to the presence of the phosphate moiety. As with other ligands, the Mn(II) interaction is greater.

That the side chain is involved in the metal binding interaction may be seen by comparison of the log K_1 values in Table II with those for 5′-AMP obtained by Khan & Martell (1967) under similar conditions. The values for pt^{6}A are about 5 log K_1 units higher.

With reference to Figure 8D, the buffer region between a = 2 and a = 3 is indicative of a disproportionation reaction according to eq 7. In this pH region, the stable 1:1 complex apparently disproportionates to a less stable 2:1 ligand–metal arrangement (Richard et al., 1959).

Discussion

We can infer from the combined NMR and potentiometric data that the binding of the metal ions with t^{6}A involves coordination with the carboxyl and probably N_6 of the side chain and either N_1 or N_7 of the adenine ring (Schweizer & Hamill, 1978). Since C_8 and C_2 as well as H_8 and H_2 displayed equivalent responses to added Mn(II), there is probably an equal distribution of complexes involving the two possible adenine ring sites.

When N_6 is substituted by a methyl group, anion formation at N_6 is no longer possible, which apparently eliminates a metal coordination site. Thus in mt^{6}A, with a lower metal–ligand complex stability constant, the metal ions apparently coordinate with the side chain nearly as well as t^{6}A, but the adenine ring binding is attenuated on the basis of the lowered sensitivity of H_8 and H_2.

Substitution of a phosphate group at the 5′ carbon of t^{6}A results in a much stronger ligand–metal complex (Table II), and the interaction with metal ion is quite specific. The combined NMR data shows that phosphorus, C_8, C_5, carbonyl, CO_2, and H_8 are primarily affected by the presence of Mn(II), with C_2 and H_2 to a much lower degree. One can construct a model encompassing these results, as shown in Figure 9. The nucleotide must be in the antiglycosidic conformation for this specific metal interaction to occur. Phosphate oxygens, along with N_7 and N_6 atoms of the adenine ring, are bound to the four corners of the octahedron, while the carboxyl group of the side chain occupies one apex and a water molecule the other.

The ligand sites of pt^{6}A are depicted in Figure 9 within the inner coordination sphere of the metal. This model is consistent with interpretations of thermodynamic data obtained from titrations at various temperatures (P. R. Reddy and M. P. Schweizer, unpublished results).

The voluminous literature on metal–purine nucleotide interactions documents involvement of a phosphate oxygen and N_7 atoms in metal binding. That N_6 may also be involved has recently been shown by Levy & Dechter (1980) for the interaction of 5′-AMP with Mn(II) using ^{15}N NMR. Combined interaction of N_7, N_6, both phosphate oxygen atoms, and the carboxyl group of pt^{6}A is consistent with the very large complex formation constants (Table II).

Although we have shown that the NMR and potentiometric results reinforce one another, it must be realized that the solution state of the ligand is not the same in the two experimental techniques. In the potentiometric determinations, the input concentrations of metal and ligands are both very low, 10^{-4} M. Thus the ligands are presumably mostly monomers. In the NMR measurements, the ligand concentrations range from 0.036 M for the ^1H NMR studies to 0.36–0.5 M for the ^{31}P and ^{13}C NMR experiments. Clearly, as shown in Figure 3, at these concentrations the ligands exist in base-stacked arrays. Despite this situation, the interaction of the one metal ion would be expected to occur with an average one or two ligands of the 2000–10 000 ligand molecules available. On the basis of the results of Kondo et al. (1970), the ligands stack in a regular array so that each ligand would be essentially equivalent.

The nature of the less strongly interacting 2:1 ligand–metal complex for pt^{6}A–Mn(II) at pD 10.3 may be visualized with reference to the ^1H NMR data and the model for the strong 1:1 complex displayed in Figure 9. Whereas in the pD 7.9 solution the H_8 proton was nearly exclusively relaxed by comparison to H_2 as Mn(II) was added, in the pD 10.3 situation the H_2 peak displays about 25% the magnitude of line broadening as does H_8. This we interpret in terms of a complex in which 75% of the metal–ligand interaction is as depicted in Figure 9 for the 1:1 interaction. The remaining 25% of complex species has one pt^{6}A molecule bound as shown in Figure 9, except only one phosphate oxygen is coordinated to the metal. In addition, a *second* pt^{6}A molecule is coordinated at two sites, carboxyl oxygen (in the metal plane) and N_1 of the adenine ring bound at the apex of the octahedron replacing water. Levy & Dechter (1980) also suggested a 2:1 ligand–metal complex as a possibility between AMP and Mn(II) at pH 10.

The results presented here on t^6A monomer ligands have definitely demonstrated the qualitative and quantitative importance of the threonine side chain involvement in the metal binding interaction, which is the distinguishing feature of this unusual nucleoside. These results do indeed establish t^6A as an efficient ligand for Mg(II) and Mn(II). Our current efforts are being directed toward study of more complicated but relevant ligands containing t^6A, including oligonucleotides and *Escherichia coli* $tRNA^{Ile}$. As a result of the very strong interaction described above, it is reasonable to speculate that specific metal–t^6A binding at the polymer level should occur and be discernible. One facet of the functional role of this type of unusual nucleoside in tRNA may be to facilitate anticodon–codon interaction through metal ion stabilization of the anticodon loop structure and/or as one ligand in a metal ion bridge between tRNA and ribosomes.

Acknowledgments

We thank Dr. David M. Grant, Dr. Charles Mayne, and staff of the NIH Regional NMR Resource, Department of Chemistry, University of Utah, for their helpful assistance. G.B.C. wishes to express appreciation for the interest and encouragement of Dr. H. C. Box.

References

Altona, C., & Sundaralingam, M. (1973) *J. Am. Chem. Soc. 95*, 2333.

Bolton, R. H., & Kearns, D. R. (1978) *Biol. Magn. Reson. 1*, 91–137.

Broom, A. D., Schweizer, M. P., & Ts'o, P. O. P. (1967) *J. Am. Soc. 89*, 3612.

Carrington, A., & McLachlan, A. D. (1967) in *Introduction to Magnetic Resonance*, pp 225–229, Harper and Row, New York.

Chheda, G. B., & Hong, C. I. (1971) *J. Med. Chem. 14*, 748.

Chheda, G. B., Hall, R. H., Magrath, D. I., Mozejko, J., Schweizer, M. P., Stasiuk, L., & Taylor, P. R. (1969) *Biochemistry 8*, 3278.

Chheda, G. B., Hong, C. I., Piskorz, C. F., & Harmon, G. (1972) *Biochem. J. 127*, 515.

Davies, D. B. (1978) *Prog. Nucl. Magn. Reson. Spectrosc. 12*, 135–225.

Dea, P., Alta, M., Patt, S., & Schweizer, M. P. (1978) *Nucleic Acids Res. 5*, 307.

Dutta, S. P., Hong, C. I., Murphy, G. P., Mittelman, A., & Chheda, G. B. (1975) *Biochemistry 14*, 3144.

Elkins, B. N., & Keller, E. B. (1974) *Biochemistry 13*, 4622.

Hall, R. H. (1971) in *The Modified Nucleosides in Nucleic Acids*, Columbia University Press, New York.

Harned, H. S., & Owen, B. B. (1959) in *Physical Chemistry of Electrolytic Solutions*, 3rd ed., p 608, Reinhold, New York.

Holbrook, S. R., Sussman, J. L., Warrant, R. W., Church, G. M., & Kim, S. H. (1977) *Nucleic Acids Res. 4*, 2811.

Hruska, F. E., Grey, A. A., & Smith, I. C. P. (1970) *J. Am. Chem. Soc. 92*, 4088.

Jack, A., Ladner, J. E., Rhodes, P., Brown, R. S., & Klug, A. (1977) *J. Mol. Biol. 111*, 315.

Karplus, W. (1959) *J. Chem. Phys. 30*, 11.

Khan, M. M. T., & Martell, A. E. (1967) *J. Am. Chem. Soc. 89*, 5585.

Kimura-Harada, F., Harada, F., & Nishimura, S. (1972a) *FEBS Lett. 21*, 71.

Kimura-Harada, F., von Minden, D. L., McCloskey, J. A., & Nishimura, S. (1972b) *Biochemistry 11*, 3910.

Kondo, N. S., Holmes, H. M., Stempel, L. M., & Ts'o, P. O. P. (1970) *Biochemistry 9*, 3479.

Korner, A., & Soll, D. (1974) *FEBS Lett. 39*, 301.

Korytnyk, W., Chheda, G. B., & Parthasarathy, R. (1976) 6th International Conference on Nuclear Magnetic Resonance, Quebec, Canada.

Lee, C. H., Ezra, F. S., Kondo, N. S., Sarma, R. H., & Danyluk, S. S. (1976) *Biochemistry 15*, 3627.

Levy, G. C., & Dechter, J. J. (1980) *J. Am. Chem. Soc. 102*, 6191.

McCloskey, J. A., & Nishimura, S. (1977) *Acc. Chem. Res. 10*, 403.

Miller, J. P., Hussain, Z., Schweizer, M. P. (1976) *Nucleic Acids Res. 3*, 1185.

Parthasarathy, R., Ohrt, J. M., & Chheda, G. B. (1974a) *J. Am. Chem. Soc. 96*, 8087.

Parthasarathy, R., Ohrt, J. M., & Chheda, G. B. (1974b) *Biochem. Biophys. Res. Commun. 60*, 211.

Powers, D. M., & Peterkofsky, A. (1972) *J. Biol. Chem. 247*, 6394.

Quigley, G. J., Teeter, M. M., & Rich, A. (1978) *Proc. Natl. Acad. Sci. U.S.A. 75*, 64.

Reddy, P. R., Schweizer, M. P., & Chheda, G. B. (1979) *FEBS Lett. 106*, 63.

Richard, C. F., Gustafson, R. L., & Martell, A. E. (1959) *J. Am. Chem. Soc. 81*, 1033.

Schwarzenbach, G. (1975) in *Complexometric Titrations*, pp 71–82, Wiley-Interscience, New York.

Schweizer, M. P., & Hamill, W. D., Jr. (1978) *Biochim. Biophys. Res. Commun. 85*, 1367.

Schweizer, M. P., Chan, S. I., Helmkamp, G. K. & Ts'o, P. O. P. (1964) *J. Am. Chem. Soc. 86*, 696.

Schweizer, M. P., Broom, A. D., Ts'o, P. O. P., & Hollis, D. P. (1968) *J. Am. Chem. Soc. 90*, 1042.

Schweizer, M. P., Chheda, G. B., Baczynskyi, L., & Hall, R. H. (1969) *Biochemistry 8*, 3283.

Schweizer, M. P., Thedford, R., & Slama, J. (1971) *Biochim. Biophys. Acta 232*, 217.

Takemura, S., Murakami, M., & Miyazaki, M. (1969) *J. Biochem. (Tokyo) 65*, 489.

Thedford, R., & Straus, D. B. (1974) *Biochemistry 13*, 535.

Watts, M. T., & Tinoco, I., Jr. (1978) *Biochemistry 17*, 2455.